Comparison between alkylrhodoximes and alkylcobaloximes. Solution studies of some alkylrhodoximes, $pyRh(DH)_2R$, and crystal structure of the complexes with $R = CH_2CF_3$, CH_2Cl, n-Pr

Lucio Randaccio*, Silvano Geremia, Renata Dreos-Garlatti, Giovanni Tauzher, Fioretta Asaro and Giorgio Pellizer

Dipartimento di Scienze Chimiche, Università di Trieste, 34127 Trieste (Italy)

(Received September 10, 1991)

Abstract

Syntheses, kinetics and NMR measurements of $pyRh(DH)_2R$ complexes, where py = pyridine and DH = monoanion of dimethylglyoxime, with various R alkyl groups are described. X-ray crystal structures of the compounds with $R = CH_2CF_3$ (**I**), CH_2Cl (**II**), n-Pr (**III**) are reported. Comparison of the geometry of the $Rh(DH)_2$ and $Co(DH)_2$ moieties shows significant differences in the M–N, N–O and O···O distances, with a decrease of the approximate symmetry from D_{2h} in cobaloximes to C_{2h} in rhodoximes. The axial Rh–C and Rh–N distances lengthen with increasing bulk and the σ-donating ability of R, respectively; the Rh–C distances are 2.059(5) Å in **I** and 2.069(5) Å in **II**, and the Rh–N(axial) distances are 2.145(3) (**I**), 2.178(3) (**II**) and 2.188(5) (**III**) Å. The chemical shifts of the pyridine *meta* and *para* carbons decrease with the increase of the alkyl group σ-donating power; the linear relationship found between the δ values of the pyridine *para* carbon in rhodoximes and the *EP* values, derived from NMR data of cobaloximes, shows that the transmission of electronic charge from R to the neutral ligand through rhodium occurs in a way similar to that through cobalt. The rate constants for the pyridine dissociation increase with the σ-donating ability of the alkyl group, as measured by *EP* parameters. These results show that, as already reported for cobaloximes, *trans*-influence and *trans*-effect have the same trend in rhodoximes too.

Introduction

Cobaloximes, $LCo(DH)_2R$ where L = neutral ligand, DH = monoanion of dimethylglyoxime and R = alkyl group, are well known and studied models of the B_{12} coenzyme (5′-deoxyadenosylcobalamin). Previous works have furnished a large amount of data [1, 2] which have provided some indications on the relative roles played by steric and electronic effects in the homolytic cleavage of the Co–C bond in the B_{12} systems [3, 4]. The availability of these data, both in solid state and in solution, allowed us to propose and to check a method to measure the σ-donating ability of the R groups by introducing the *EP* parameter, derived from NMR data [5, 6]. To obtain further insight into the relative importance of steric and electronic effects, we have recently reported a preliminary study of some $LRh(DH)_2R$ complexes (alkylrhodoximes) [7]. The structural results have suggested weaker steric interaction between axial and equatorial ligands and less 'hindered' coordination around the metal atom than in the corresponding cobaloximes [7]. In order to get a better understanding of these aspects we have examined the NMR spectra of rhodoximes. Moreover, since the previous structural and kinetic results were restricted to alkylrhodoximes having σ-donating alkyl groups, the investigation has been extended to other derivatives having electron withdrawing R groups such as CH_2CF_3 and CH_2Cl, to widen the study of the *trans*-steric effect and influence [5, 8].

*Author to whom correspondence should be addressed.

Experimental

Synthesis

The organorhodium complexes $pyRh(DH)_2R$, where R = Me, Et, i-Pr, n-Pr, CH_2CF_3, CH_2Cl, were prepared by the procedure previously described [7]. Crystals of the n-Pr, CH_2CF_3 and CH_2Cl derivatives suitable for X-ray analysis were prepared by slow diffusion of a layer of n-pentane into a saturated CH_2Cl_2 solution of the complex at room temperature. The organocobalt complexes were prepared according to published procedures [2]. All other materials were reagent grade and were used without further purification.

0020-1693/92/$5.00

Kinetic measurements

Ligand substitution reactions were monitored spectrophotometrically in the range 350–450 nm using a Uvikon 940 instrument. Kinetic runs were carried out in CH_2Cl_2 at 25 °C, under pseudo first order excess of entering ligand, with concentrations ranging from 4×10^{-3} to 5×10^{-1} M. Generally, 2 to 4×10^{-4} M concentrations of the complex were used. The observed rate constants, k_{obs}, were obtained from a linear plot of $\ln(A-A_\infty)$ versus time, where A is the absorbance at time t and A_∞ is the final absorbance.

NMR measurements

Spectra were recorded in deuterochloroform solutions at 80 MHz for proton and 20.1 MHz for carbon, with a Bruker WP 80 spectrometer, equipped with an ASPECT 2000 computer.

For ^1H spectra TMS was used as the internal standard, spectral width was 1000 Hz, digital resolution 0.125 Hz/pt, flip angle 90°, delay between pulses 10 s.

For ^{13}C spectra TMS was used as the internal standard, spectral width was 6000 Hz, digital resolution 0.375 Hz/pt, flip angle 30°. Proton decoupling was made through broad-band irradiation. Assignment of resonances in $\{^1H\}^{13}C$ NMR spectra, where not straightforward, was defined by means of gated undecoupled spectra or of the usual pulse sequence for quaternary carbons only detection (QUATD.AU).

Crystal data, data collections and processing

Cell dimensions were obtained by least-squares refinement from 25 reflections lying in the θ range 15–21°, using graphite-monochromated Mo Kα radiation ($\lambda=0.7107$ Å), on an Enraf-Nonius CAD4 single-crystal diffractometer. Reflections with $I\geqslant3\sigma(I)$ were corrected for Lorentz and polarization effects. Empirical absorption corrections based on Ψ-scan data and secondary extinction were not applied to the reflection intensities only for compound **III** because of the small size and cubic form of the crystal and of the low μ value. Crystal data and some details of data collections are summarized in Table 1.

Solution and refinement of the structures

All the structures were solved by conventional Patterson and Fourier methods. The Fourier and difference Fourier maps of the structure **III** clearly showed a disordered n-Pr group. The relative electron density peaks were interpreted successfully by assuming three different orientations of the n-Pr group having occupancies 0.5, 0.25 and 0.25. The two orientations with occupancy 0.25 are related to that with occupancy 0.5, shown in the ORTEP drawing, by a rotation of $\pm80°$ around an axis passing through Rh and normal to the equatorial coordination plane. The occupancies were fixed on the basis of the height of the electron density peaks on the Fourier map. H atoms, at calculated geometrical positions, were located on a difference Fourier map. Final full-matrix anisotropic least-squares refinements, with the fixed contribution of hydrogen atoms ($B=1.3\times B_{eq}$ of the atom they are attached) and of the n-Pr disordered group ($B=6$ Å^2 for C atoms) for **III**, converged to the R and R_w values reported in Table 1. The unitary weighting scheme gave satisfactory agreement analyses. Anomalous dispersion was applied. The refinements with the signs of *if*'' reversed (or with inverted coordinates) gave $R_w^-=0.030$ and 0.042 for **I** and **III**, respectively. The values $R_w^-/R_w^+=1.15$ (**I**)

TABLE 1. Crystallographic data for compounds **I–III** ($pyRh(DH)_2R$). All data collected at 18 °C using graphite-monochromated Mo Kα radiation ($\lambda=0.7107$ Å)

	I	**II**	**III**
R	CH_2CF_3	CH_2Cl	$CH_2CH_2CH_3$
Formula	$RhF_3O_4N_5C_{15}H_{21}$	$RhClO_4N_5C_{14}H_{21}$	$RhO_4N_5C_{16}H_{26}$
Formula weight	495.3	461.7	455.3
a (Å)	9.838(2)	9.073(2)	9.750(2)
b (Å)	15.958(2)	14.7868(8)	12.628(2)
c (Å)	12.500(2)	14.064(3)	16.063(6)
β (°)	92.733(8)	94.97(1)	
V (Å^3)	1960.2(5)	1879.7(7)	1977.8(9)
Z	4	4	4
Space group	$P2_1$ (No. 4)	$P2_1/n$ (No. 14)	$P2_12_12_1$ (No. 19)
D_{calc} (g cm^{-3})	1.68	1.63	1.53
D_{meas} (g cm^{-3})	1.70	1.65	1.55
μ (Mo Kα) (cm^{-1})	9.1	10.6	8.8
No. measured reflections	6142	5885	3259
No. independent reflections ($I\geqslant3\sigma(I)$)	5434	3792	2414
$R(F_o)$	0.024	0.042	0.039
$R_w(F_o)$	0.026	0.041	0.039

and 1.08 (III) confirm the correct assignment of the absolute configuration for the non-centrosymmetric structures I and III [9]. Final non-hydrogen positional parameters and B_{eq} (Å^2) are given in Tables 2–4. Atomic scattering factors, anomalous dispersion terms, and programs were taken from the Enraf-Nonius SDP package [10]. See also 'Supplementary material'.

Results and discussion

Rate measurement

The k_{obs} values for the substitution reactions

$$pyRh(DH)_2R + PPh_3 \rightleftharpoons PPh_3Rh(DH)_2R + py$$

($R = CH_2CF_3$ and CH_2Cl) are independent of [PPh_3] in the examined concentrations range, as expected for a D mechanism, which has been proved previously to be operative in the ligand exchange reactions of organorhodoximes [7, 11], and organocobaloximes [2, 12] in CH_2Cl_2. In fact for a D mechanism

$$X\text{–}M\text{–}L \underset{k_{-1}}{\overset{k_1}{\rightleftharpoons}} X\text{–}M + L$$

$$X\text{–}M + L' \underset{k_{-2}}{\overset{k_2}{\rightleftharpoons}} X\text{–}M\text{–}L'$$

where M represents the central metal ion with the equatorial ligands and X the non-labile axial group, the expression

$$k_{obs} = \frac{k_1 + k_{-2}k_{-1}[L]/k_2[L']}{1 + k_{-1}[L]/k_2[L']}$$

reduces to

$$k_{obs} = k_1 \qquad (1)$$

in the absence of added leaving ligand, so that the reaction rate becomes independent of both concentration and chemical identity of L'. The py dissociation rate constants k_1 are reported in Table 5.

NMR spectra

Selected values of NMR parameters are reported in Tables 6 and 7.

TABLE 2. Atomic positional parameters and their e.s.d.s for compound I

Atom	x	y	z	B_{eq}[a] (Å^2)	Atom	x	y	z	B_{eq}[a] (Å^2)
Molecule A					Molecule B				
RhA	0.49207(2)	0.75	0.86329(2)	3.128(4)	RhB	0.98995(2)	0.25964(2)	0.64387(2)	3.467(5)
F1A	0.5404(4)	0.9080(2)	0.5884(3)	7.90(9)	F1B	0.8750(4)	0.0808(2)	0.7696(3)	8.36(9)
F2A	0.6720(3)	0.8985(2)	0.7314(3)	8.4(1)	F2B	0.9973(4)	0.0946(3)	0.9160(3)	9.0(1)
F3A	0.6449(3)	0.7931(2)	0.6236(2)	8.05(8)	F3B	0.8487(4)	0.1903(3)	0.8731(3)	8.9(1)
O1A	0.2005(3)	0.7166(2)	0.8210(2)	4.92(7)	O1B	0.6987(3)	0.2790(2)	0.6859(2)	5.57(7)
O2A	0.6040(3)	0.8812(2)	1.0003(2)	4.35(6)	O2B	1.1018(3)	0.1335(2)	0.5082(3)	5.12(7)
O3A	0.7842(3)	0.7833(2)	0.9076(3)	5.18(7)	O3B	1.2755(3)	0.2378(2)	0.5956(2)	5.00(7)
O4A	0.3827(3)	0.6166(2)	0.7296(2)	4.43(6)	O4B	0.8824(3)	0.3900(2)	0.7764(2)	4.76(6)
N1A	0.2935(3)	0.7670(2)	0.8747(2)	3.74(6)	N1B	0.7933(3)	0.2308(2)	0.6357(3)	4.29(7)
N2A	0.4888(3)	0.8488(2)	0.9600(3)	3.49(6)	N2B	0.9877(4)	0.1607(2)	0.5473(3)	4.22(7)
N3A	0.6905(3)	0.7330(2)	0.8524(3)	3.92(7)	N3B	1.1863(3)	0.2867(2)	0.6500(3)	3.90(7)
N4A	0.4971(3)	0.6508(2)	0.7670(3)	3.80(6)	N4B	0.9942(3)	0.3594(2)	0.7389(3)	3.67(6)
N5A	0.4955(3)	0.6710(2)	1.0022(3)	3.62(6)	N5B	0.9516(3)	0.3394(2)	0.5076(3)	3.74(6)
C1A	0.1099(4)	0.8491(4)	0.9522(4)	5.0(1)	C1B	0.6090(5)	0.1478(4)	0.5486(4)	6.1(1)
C2A	0.2560(4)	0.8285(3)	0.9337(3)	3.73(7)	C2B	0.7562(5)	0.1704(3)	0.5731(3)	4.51(9)
C3A	0.3685(4)	0.8768(3)	0.9841(3)	3.66(7)	C3B	0.8699(5)	0.1284(3)	0.5230(4)	4.54(9)
C4A	0.3486(5)	0.9494(3)	1.0572(4)	4.92(9)	C4B	0.8512(6)	0.0526(3)	0.4523(4)	6.0(1)
C5A	0.8749(4)	0.6460(4)	0.7871(5)	5.9(1)	C5B	1.3712(4)	0.3777(4)	0.7182(4)	5.7(1)
C6A	0.7292(4)	0.6703(3)	0.7979(4)	4.08(8)	C6B	1.2253(4)	0.3498(3)	0.7072(3)	3.94(8)
C7A	0.6159(4)	0.6232(3)	0.7451(3)	3.81(8)	C7B	1.1165(4)	0.3922(3)	0.7611(3)	3.77(7)
C8A	0.6401(5)	0.5509(3)	0.6708(4)	4.68(9)	C8B	1.1373(5)	0.4651(3)	0.8340(4)	5.0(1)
C9A	0.4659(5)	0.8273(3)	0.7321(4)	5.1(1)	C9B	1.0426(5)	0.1840(4)	0.7728(4)	5.6(1)
C10A	0.5765(5)	0.8546(4)	0.6686(4)	6.1(1)	C10B	0.9437(7)	0.1399(4)	0.8326(5)	6.9(1)
C11A	0.4096(4)	0.6068(3)	1.0079(4)	4.48(9)	C11B	0.8525(5)	0.3962(3)	0.5038(4)	4.60(9)
C12A	0.4016(5)	0.5572(3)	1.0975(4)	5.4(1)	C12B	0.8230(5)	0.4461(3)	0.4169(4)	5.7(1)
C13A	0.4858(6)	0.5739(4)	1.1849(4)	6.0(1)	C13B	0.9004(6)	0.4386(4)	0.3283(4)	6.3(1)
C14A	0.5706(6)	0.6404(4)	1.1806(4)	6.7(1)	C14B	1.0044(6)	0.3825(4)	0.3313(4)	6.3(1)
C15A	0.5763(5)	0.6865(3)	1.0883(4)	5.5(1)	C15B	1.0273(5)	0.3327(4)	0.4219(4)	5.0(1)

[a]Values for anisotropically refined atoms are given in the form of the isotropic equivalent displacement parameter defined as $B_{eq} = (4/3)\Sigma_i\Sigma_j a_i a_j \beta(i, j)$.

TABLE 3. Atomic positional parameters and their e.s.d.s for compound **II**

Atom	x	y	z	B_{eq}[a] (Å^2)	Atom	x	y	z	B_{eq}[a] (Å^2)
Rh	−0.00851(3)	0.16441(2)	0.24338(3)	3.619(5)	C3	0.0513(5)	0.3284(3)	0.1522(4)	4.6(1)
Cl	0.3300(2)	0.1350(2)	0.3359(2)	12.45(6)	C4	0.1032(7)	0.3940(4)	0.0812(5)	7.3(2)
O1	−0.1643(4)	0.2943(2)	0.3521(2)	4.90(7)	C5	0.0557(7)	−0.1204(4)	0.2308(6)	7.6(2)
O2	0.1580(4)	0.2076(3)	0.0791(3)	6.34(9)	C6	0.0235(5)	−0.0242(3)	0.2564(4)	5.1(1)
O3	0.1406(4)	0.0348(3)	0.1312(3)	6.30(9)	C7	−0.0629(5)	0.0003(3)	0.3361(4)	4.8(1)
O4	−0.1692(4)	0.1210(3)	0.4092(2)	5.36(8)	C8	−0.1127(7)	−0.0675(4)	0.4057(4)	6.5(1)
N1	−0.0805(4)	0.2857(2)	0.2797(3)	3.93(7)	C9	0.1690(6)	0.1910(4)	0.3419(4)	6.0(1)
N2	0.0782(4)	0.2425(3)	0.1482(3)	4.59(8)	C10	−0.3374(5)	0.1711(3)	0.1727(3)	4.34(9)
N3	0.0642(4)	0.0438(3)	0.2067(3)	4.82(9)	C11	−0.4662(5)	0.1620(4)	0.1133(4)	5.2(1)
N4	−0.0906(4)	0.0867(3)	0.3401(3)	4.23(8)	C12	−0.4611(6)	0.1223(4)	0.0265(4)	5.4(1)
N5	−0.2065(4)	0.1438(2)	0.1467(2)	3.62(7)	C13	−0.3287(6)	0.0929(4)	0.0001(4)	5.7(1)
C1	−0.0691(6)	0.4501(4)	0.2551(4)	5.8(1)	C14	−0.2040(5)	0.1049(4)	0.0612(3)	4.8(1)
C2	−0.0359(5)	0.3541(3)	0.2305(3)	4.25(9)					

[a]See footnote of Table 2.

TABLE 4. Atomic positional parameters and their e.s.d.s for compound **III**

Atom	x	y	z	B_{eq}[a] (Å^2)	Atom	x	y	z	B_{eq}[a] (Å^2)
Rh	0.24712(6)	0.13242(3)	0.24160(2)	3.221(6)	C7	0.0110(7)	0.0612(5)	0.3244(4)	3.7(1)
O1	0.1357(5)	0.2648(4)	0.1115(3)	4.2(1)	C8	−0.1368(8)	0.0399(7)	0.3474(5)	5.2(2)
O2	0.5397(4)	0.0934(4)	0.2709(3)	4.7(1)	C12	0.143(1)	−0.0126(7)	0.0993(5)	5.5(2)
O3	0.3634(5)	0.0004(4)	0.3709(3)	3.94(9)	C13	0.130(1)	−0.1016(8)	0.0504(5)	7.5(3)
O4	−0.0461(5)	0.1727(4)	0.2150(3)	5.1(1)	C14	0.209(2)	−0.1861(7)	0.0659(6)	9.8(4)
N1	0.2501(7)	0.2304(3)	0.1443(3)	3.45(8)	C15	0.304(1)	−0.1839(7)	0.1278(6)	9.2(3)
N2	0.4457(5)	0.1461(4)	0.2200(3)	3.7(1)	C16	0.314(1)	−0.0894(7)	0.1731(6)	6.9(2)
N3	0.2480(7)	0.0367(3)	0.3397(3)	3.30(8)	C9A	0.2584	0.2459	0.3354	[b]
N4	0.0487(5)	0.1216(4)	0.2648(3)	3.7(1)	C10A	0.2443	0.3632	0.3105	[b]
N5	0.2332(7)	−0.0066(4)	0.1607(3)	3.7(1)	C11A	0.2472	0.4319	0.3898	[b]
C1	0.3908(8)	0.3321(6)	0.0452(4)	4.3(2)	C9B	0.2793	0.2715	0.3125	[b]
C2	0.3706(7)	0.2556(5)	0.1159(4)	3.5(1)	C10B	0.1506	0.3362	0.3344	[b]
C3	0.4855(7)	0.2053(5)	0.1612(4)	3.5(1)	C11B	0.1971	0.4316	0.3872	[b]
C4	0.6298(8)	0.2230(6)	0.1369(6)	5.2(2)	C9C	0.2238	0.2619	0.3206	[b]
C5	0.1045(8)	−0.0593(6)	0.4433(5)	4.9(2)	C10C	0.3484	0.3353	0.3333	[b]
C6	0.1250(8)	0.0127(5)	0.3699(4)	4.0(1)	C11C	0.3027	0.4337	0.3828	[b]

[a]See footnote of Table 2. [b]Atom with partial occupancy not refined, see text.

TABLE 5. Values of $\log k_1$ for 4CN-pyCo(DH)$_2$R and pyRh(DH)$_2$R, differences in chemical shifts, $\delta_{Me} - \delta_R$, for py *para* carbons of pyRh(DH)$_2$R, and *EP* parameters

R	$\log k_1$(Co)	$\log k_1$(Rh)	$\delta_{Me} - \delta_R$	*EP*
CH_2CF_3	−3.57[a]	−4.87[b]	-0.6_3[b]	−0.53[c]
CH_2Cl	−2.51[a]	−3.11[b]	-0.4_9[b]	−0.35[c]
Me	−1.39[a]	−1.48[d]	0.00	0.00[c]
Et	−0.02[a]	−0.24[d]	0.1_3[b]	0.15[c]
n-Pr	0.08[a]	−0.27[d]	0.1_3[b]	0.18[c]
i-Pr	1.43[a]	0.80[d]	0.2_3[b]	0.30[c]

[a]Ref. 2. [b]Present work. [c]Ref. 5. [d]Ref. 7. [e]Ref. 6.

Substituting Rh(III) for Co(III) in pyridinoalkylcobaloximes causes a strong shielding on the axial alkyl carbon bonded to the metal [15], and much poorer effects on all the other carbons. Noticeably, all the axial ligands atoms in β position to the metal are 0.5–0.9 ppm more shielded.

The α substituent effects of the pyRh(DH)$_2$ moieties on *R* (differences between the C-α chemical shifts in pyRh(DH)$_2$R and in HR [15] are 1.5, 8.7, 8.4, 12.3 ppm for R = Me, Et, n-Pr and i-Pr; they increase with increasing the steric interaction between the axial and the equatorial ligands as reflected by the Rh–C bond lengths (see Table 9). A parallel trend was found in the analogous pyridinoalkylcobaloximes, the effects being 13.3, 18.3, 18.5 and 21.3 ppm, respectively [15]. The substituent effects on the β carbons (8.4, 6.8 and 9.5 for R = Et, n-Pr and i-Pr, respectively) lead to values and a trend similar to the ones of the cobalt analogues [13]. Those on the α hydrogens are still deshielding but much smaller.

Specially important in these alkylrhodoximes is the progressive deshielding of the *meta* and *para* pyridine

TABLE 6. ^{13}C NMR data for $pyRh(DH)_2R$ and py. ^{13}C δ values in ppm from TMS; coupling constants (Hz) in parentheses

R	py			DH		R		
	C *ortho*	C *meta*	C *para*	C=N	CH_3	C-α	^1J(Rh, C)	C-β
$pyRh(DH)_2R$								
CH_2CF_3	149.5	125.8	138.3	150.5	11.8	12.9	(28)	132.0
CH_2Cl	149.7	125.7	138.1	150.3	11.9	38.8	(30)	
Me	149.6_5	125.5	137.6	149.5	11.8	−0.6	(23)	
Et	149.6	125.4	137.5	149.2	11.8	15.2	(23)	14.9
n-Pr	149.6	125.4	137.5		11.8	24.5	(23)	23.1
i-Pr	149.6	125.3	137.4	149.3	11.9	28.6	(23)	25.6
$pyCo(DH)_2R$								
CH_2CF_3	149.9	125.4	138.0	150.8	12.2	bs		132.0
Me	150.0	125.2	137.5	149.0	12.0	bs		
py[a]	150.0	124.0	136.2					

[a]Ref. 13.

TABLE 7. ^1H Chemical shifts for $pyRh(DH)_2R$ and py (ppm from TMS)

R	py			DH	R	
	H *ortho*	H *meta*	H *para*	CH_3	H-α	H-β
$pyRh(DH)_2R$						
CH_2CF_3	8.47	7.33	7.77	2.11	1.33	
CH_2Cl	8.47	7.33	7.76	2.15	3.58	
Me	8.50	7.31	7.73	2.14	0.28	
Et	8.47	7.30	7.73	2.14	1.27	0.59
n-Pr	8.47	7.29	7.71	2.14		
i-Pr	8.47	7.28	7.70	2.13	1.47	0.77
py[a]	8.58	7.23	7.63			

[a]Ref. 14.

carbons and protons, associated with the decrease of the electrondonating ability of R. This behaviour indicates a diminution of the electron density at the *meta* and *para* positions.

The direct carbon–hydrogen coupling constants of the pyridine are larger in the CH_2CF_3 cobalt and rhodium derivatives than in the free ligand, the difference being 9 Hz for the *ortho* and 5 Hz for the *meta* and *para* positions. Comparison with pyridine-*N*-oxide and pyridinium [16] suggests that the metal–pyridine interaction in these complexes is rather strong.

Structural studies

The rhodium atom has a distorted octahedral coordination in all the three rhodoximes, as shown by the ORTEP drawings for non-hydrogen atoms depicted in Figs. 1–3, together with the atom numbering scheme. For I, the numbering scheme refers to one of the two crystallographically independent molecules, A, and applies also to molecule B. Figure 3 shows only the n-Pr group with the highest occupancy. The two chemically equivalent halves of the equatorial ligand are approximately planar and α, the corresponding dihedral angle between their mean planes, is reported in Table 8 together with d, the displacement of the Rh atom out of the mean plane passing through the four equatorial N-donor atoms. In previous papers, regarding $LCo(DH)_2R$ complexes [1, 2], it has been assumed that bendings toward the alkyl group and displacements

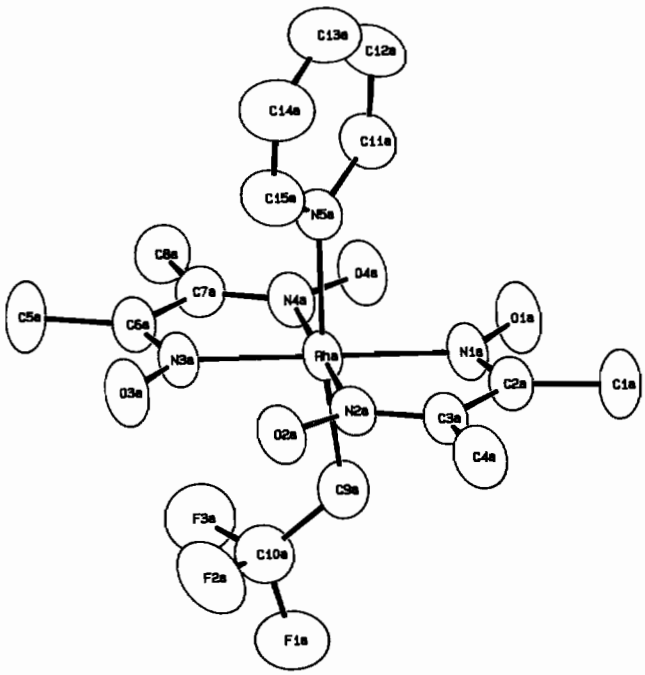

Fig. 1. ORTEP drawing (50% probability thermal ellipsoids) and labeling scheme for non-hydrogen atoms of molecule A of I. The same scheme applies also for B.

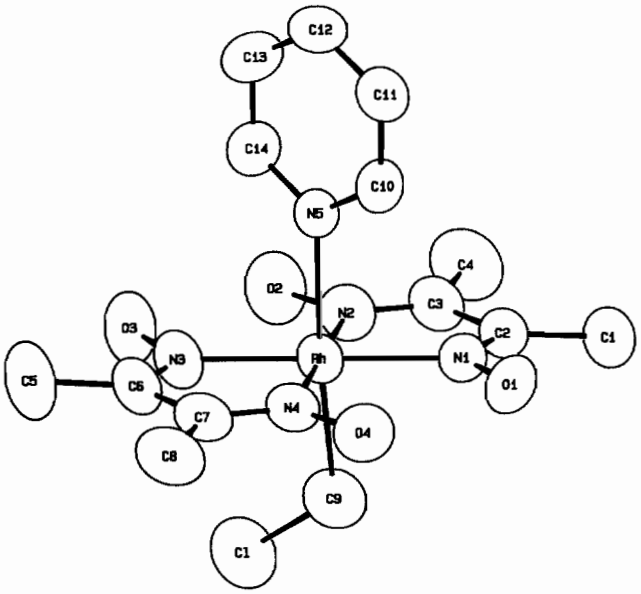

Fig. 2. ORTEP drawing (50% probability thermal ellipsoids) and labeling scheme for non-hydrogen atoms of **II**.

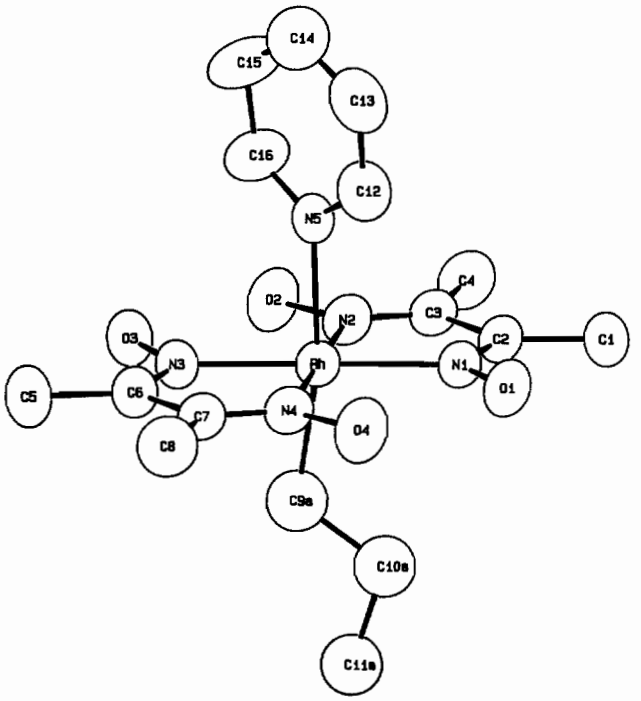

Fig. 3. ORTEP drawing (50% probability thermal ellipsoids) and labeling scheme for non-hydrogen atoms of **III**. Only the orientation of the n-Pr group of higher occupancy is shown.

toward the neutral ligand are denoted by positive values of α and d, respectively.

In **I–III** the py plane crosses the oxime bridges with an orientation very close to that found in py cobaloximes, and in py rhodoximes with R = Et, i-Pr [7], but different from that reported for $pyRh(DH)_2Me$, where the py plane crosses the two five-membered rings of the $Rh(DH)_2$ moiety [7]. The geometry of the axial fragment for **I–III** is listed in Table 8. Mean values of bond lengths and angles of the equatorial moiety for rhodoximes are reported in Fig. 4.

Equatorial moiety

Beside the expected variations due to the different size of the metal centres, i.e. in the M–N(equatorial) and the O···O oxime bridge distances, and in the bond angles [7], the comparison of the equatorial moieties reveals an interesting dissimilarity between alkylrhodoximes and alkylcobaloximes. The averages over some hundred measurements of each bond length and angle of the cobaloximes equatorial moiety showed an approximately D_{2h} symmetry [2]. A similar study for all the available Rh complexes*, indicates that the approximate symmetry is lowered to C_{2h} (Fig. 4). The increase of the O···O distance on going from Co to Rh complexes is accompanied by a significant difference in the N–O distances. The longer N–O distance is that involving the O bearing the H atom (Fig. 4). An analogous effect, observed in the enol form of the β-diketones, was attributed to the different hydrogen bond force [18, 19].

Axial ligands

In a previous paper [7] we have shown that the coordination is less crowded around Rh than around Co, so that in the series $pyM(DH)_2R$, with M = Co, Rh and R = Me, Et, i-Pr, the Rh–R bond lengths increase with the increasing bulk of R significantly less than the Co–R analogues. We show now that this finding holds also when the R group is a poorer σ-donating group such as CH_2CF_3 and CH_2Cl (Table 9). The slope 0.56 in the linear regression plot (Fig. 5) of the Rh–C distances for a series $pyRh(DH)_2R$ versus the Co–C distances for the analogues cobaloximes (Table 9) confirms that the variation in metal-carbon bond length is smoother for Rh than for Co.

The Rh–py distances (Table 8) are influenced mainly by the σ-donating power of the *trans* alkyl group, ranging from 2.144(3) Å when $R = CH_2CF_3$ to 2.230(4) Å when R = i-Pr. Furthermore the M–N(axial) bond distance longer in rhodoximes than in cobaloximes is in agreement with the trend suggested for the torsional barrier around the M–py bond, Rh < Co [20].

*The available structures with R index below 0.05: $pyRh(DH)_2CH_2CF_3$[a,b], $pyRh(DH)_2CH_2Cl$[a], $pyRh(DH)_2$n-Pr[a], $pyRh(DH)_2$i-Pr[c], $pyRh(DH)_2Me$[c], $pyRh(DH)_2Et$[c,d], $pyRh(DH)_2Cl$[e], $ClRh(DH)_2Cl^-$[f], and $NH_3Rh(DH)_2NH_3^+$[f], were utilized in the calculations. The averages were calculated by weighting each measurement by the inverse square of its individual standard deviations ([a]Present work. [b]Two independent molecules. [c]Ref. 7. [d]One of the two independent molecules with large distortion in oxime bridge was rejected. [e]Unpublished results from this laboratory. [f]Ref. 17.)

TABLE 8. Bond lengths (Å) and angles (°) of the axial fragment, py–Rh–R, of **I–III**. The displacements d (Å), and the bending angles, α (°) are also reported

R	Rh–N	Rh–C	N–Rh–C	Rh–C–X	C(ax)–X	d	α
CH_2CF_3(A)	2.144(3)	2.058(5)	173.6(2)	123.4(3)	1.445(7)	−0.002	−2.6
CH_2CF_3(B)	2.146(3)	2.060(5)	175.6(2)	122.8(4)	1.438(8)	+0.007	−3.8
CH_2Cl	2.178(3)	2.069(5)	175.2(2)	120.0(3)	1.688(6)	+0.012	+0.8
n-Pr	2.188(5)					+0.019	+1.5

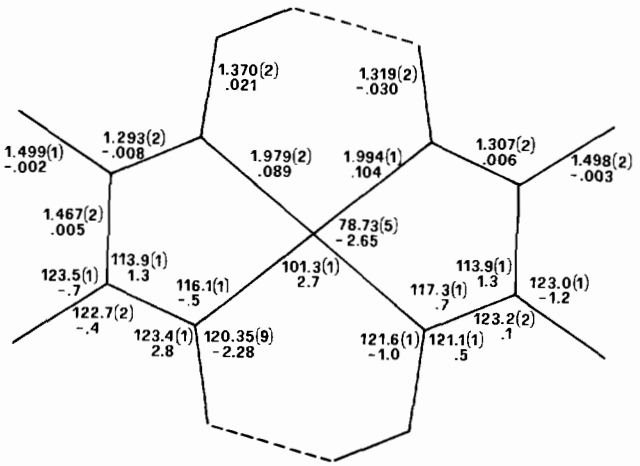

Fig. 4. Mean values of the chemically equivalent bond lengths (Å) and angles (°) (e.s.d.s in parentheses) for $Rh(DH)_2$ equatorial moiety. The differences with cobaloximes are reported for comparison.

TABLE 9. Rh–C bond lengths (Å) in $pyRh(DH)_2R$ and Co–C bond lengths (Å) in analogous cobaloximes

R	Rh–C	Co–C
CH_2CF_3	2.059(5)[a,b]	2.010(3)[c,d]
CH_2Cl	2.069(5)[a]	2.029(5)[e]
Me	2.063(5)[f]	1.998(5)[c]
Et	2.079(3)[b,f]	2.035(5)[c,g]
i-Pr	2.107(5)[f]	2.085(3)[c]

[a]Present work. [b]Mean values. [c]Ref. 2. [d]4CN–py-$Co(DH)_2CH_2CF_3$. [e]$PPh_3Co(DH)_2CH_2Cl$, unpublished results from this laboratory. [f]Ref. 7. [g]4N(H)=C(OMe)–pyCo-$(DH)_2Et$.

The difference in chemical shifts, $\delta_{Me}-\delta_R$, for the *para* carbon atom of the pyridine, given in Table 5, is plotted in Fig. 6 against the *EP* parameter (Table 5), which is essentially derived from the corresponding chemical shift difference in pyridine cobaloximes. The linear relationship with slope close to unity (correlation coefficient $r=0.994$), indicates that the transmission of the electronic charge between the axial ligands through the metal centre in the rhodoximes is modulated by the σ-donating ability of R in a way similar to that of the cobaloximes [2].

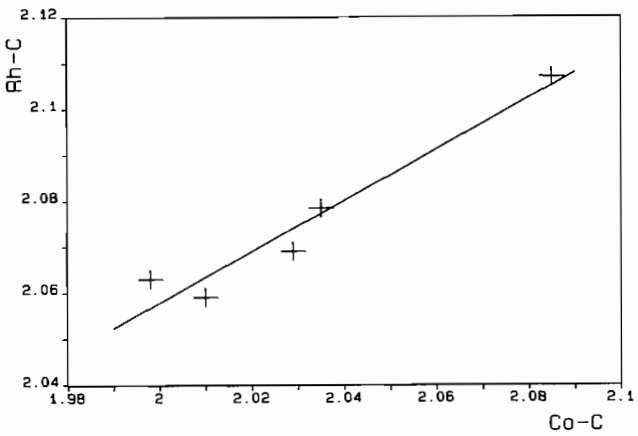

Fig. 5. Rh–C bond lengths (Å) vs. Co–C bond lengths (Å).

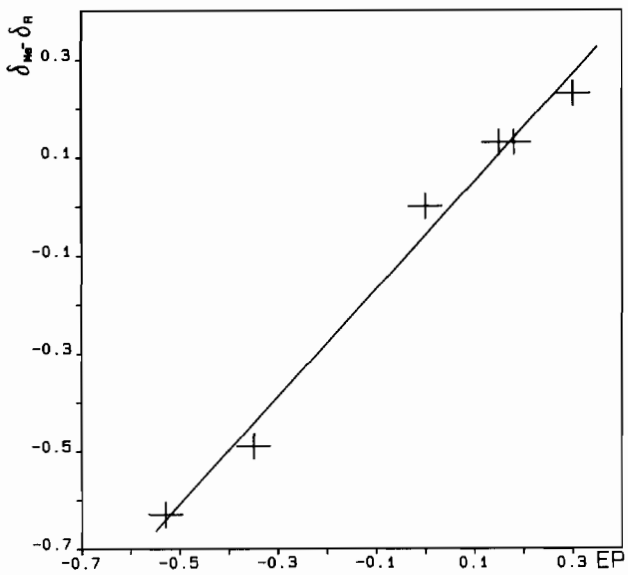

Fig. 6. Difference in chemical shifts, $\delta_{Me}-\delta_R$, for *para* carbon atoms of py vs. *EP*.

The plots of $\log k_1$ for Rh and Co complexes against *EP*, derived from data of Table 5, are given in Fig. 7. The corresponding best fit equations are:

$$\log k_1(\mathrm{Rh}) = 6.4(4)\times EP - 1.3(3) \quad r=0.993 \qquad (1)$$

$$\log k_1(\mathrm{Co}) = 5.5(6)\times EP - 0.8(4) \quad r=0.977 \qquad (2)$$

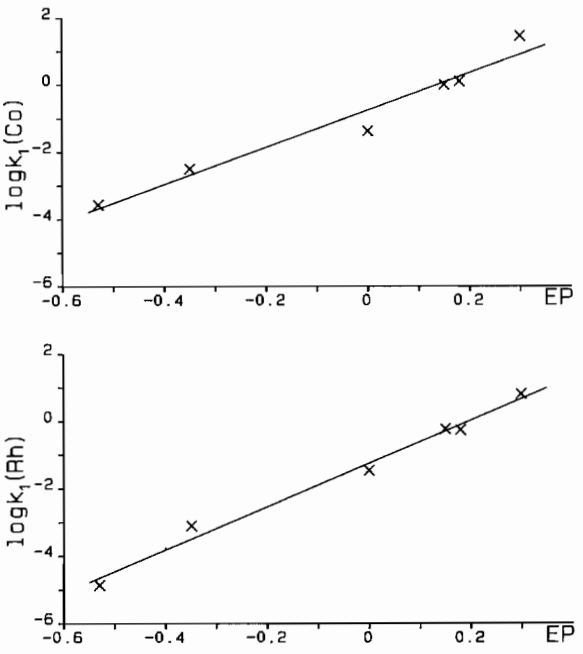

Fig. 7. Plots of $\log k_1$(Co) and $\log k_1$(Rh) vs. *EP*.

The correlation coefficient r is closer to unity in rhodoximes than in cobaloximes. As already noticed, the largest deviations from linearity in alkylcobaloximes are observed with the bulkiest alkyl group [5], which force the equatorial ligands to bend towards py and facilitate its dissociation (steric *trans*-effect) [5]. This comparison supports the point of view [7] that steric effects are less important in determining the properties of the M–N(axial) bond for rhodoximes than for cobaloximes.

Supplementary material

Hydrogen atom coordinates, anisotropic thermal parameters and tables of all the bond lengths and angles and tables of observed and calculated structure factors are available from the authors on request.

Acknowledgements

We are grateful to CNR (Rome) and to MURST (Rome) for financial support.

References

1 L. Randaccio, N. Bresciani Pahor, E. Zangrando and L. G. Marzilli, *Chem. Soc. Rev., 18* (1989) 225.
2 N. Bresciani Pahor, M. Forcolin, L. G. Marzilli, L. Randaccio, M. F. Summers and P. J. Toscano, *Coord. Chem. Rev., 63* (1985) 1, and refs. therein.
3 S. H. Kim, L. H. Chen, N. Feilchenfeld and J. Halpern, *J. Am. Chem. Soc., 110* (1988) 3120; B. P. Hay and R. G. Finke, *J. Am. Chem. Soc., 109* (1987) 8012; J. M. Pratt, *Chem. Soc. Rev., 14* (1985) 161; B. T. Golding, *J. R. Neth. Chem. Soc., 106* (1987) 342.
4 J. Halpern, *Science, 227* (1985) 869; V. B. Pett, M. N. Liebman, P. Murray-Rust, K. Prasad and J. P. Glusker, *J. Am. Chem. Soc., 109* (1987) 3207.
5 N. Bresciani Pahor, S. Geremia, C. Lopez, L. Randaccio and E. Zangrando, *Inorg. Chem., 29* (1990) 1043.
6 E. Zangrando, N. Bresciani Pahor, L. Randaccio, J. P. Charland and L. G. Marzilli, *Organometallics, 5* (1986) 1938.
7 N. Bresciani Pahor, R. Dreos Garlatti, S. Geremia, L. Randaccio, G. Tauzher and E. Zangrando, *Inorg. Chem., 29* (1990) 3437.
8 S. Geremia, M. Mari, L. Randaccio and E. Zangrando, *J. Organomet. Chem., 408* (1991) 95.
9 D. Rogers, *Acta Crystallogr., Sect. A, 37* (1981) 734.
10 B. A. Frenz, *Enraf-Nonius Structure Determination Package,* Version 18, Enraf-Nonius, Delft, Netherlands.
11 R. Dreos Garlatti and G. Tauzher, *Polyhedron, 29* (1990) 3437.
12 R. C. Stewart and L. G. Marzilli, *J. Am. Chem. Soc., 100* (1978) 817.
13 A. Marker, A. J. Canty and R. T. C. Brownlee, *Aust. J. Chem., 31* (1978) 1255.
14 H. A. O. Hill and K. G. Morallee, *J. Chem. Soc. A,* (1979) 554.
15 C. Bied-Charreton, B. Septe and A. Gaudemer, *Org. Magn. Reson., 7* (1975) 116.
16 H. O. Kalinowski, S. Berger and S. Braun, *Carbon-13 NMR Spectroscopy,* Wiley, Chichester, UK, 1988.
17 Yu. A. Simonov, L. A. Nemchinova, A. V. Ablov, V. E. Zavodnik and O. A Bologa, *Zh. Strukt. Khim., 17* (1976) 142.
18 G. Gilli, F. Bellucci, V. Ferretti and V. Bertolasi, *J. Am. Chem. Soc., 111* (1989) 1023.
19 J. Emsley, *Structure and Bonding,* Vol. 57, Springer, Berlin, 1984, p. 147.
20 J. Huet and A. Gaudemer, *Org. Magn. Reson., 15* (1981) 347.